

Facile and Versatile Strategy for Construction of Anti-Inflammatory and Antibacterial Surfaces with Polydopamine-Mediated Liposomes Releasing Dexamethasone and Minocycline for Potential Implant Applications

Xiao Xu,[†] Lixin Wang,^{*,‡} Zuyuan Luo,[§] Yaofeng Ni,[‡] Haitao Sun,[‡] Xiang Gao,^{||} Yongliang Li,[†] Siqi Zhang,[§] Yan Li,[§] and Shicheng Wei^{*,†,§,||}

[†]Central Laboratory/Department of Oral and Maxillofacial Surgery, Peking University School and Hospital of Stomatology, National Engineering Laboratory for Digital and Material Technology of Stomatology, Beijing Key Laboratory of Digital Stomatology, Beijing 100081, P. R. China

[‡]Department of Stomatology, Beijing Shijitan Hospital, Capital Medical University, Beijing 100038, P. R. China

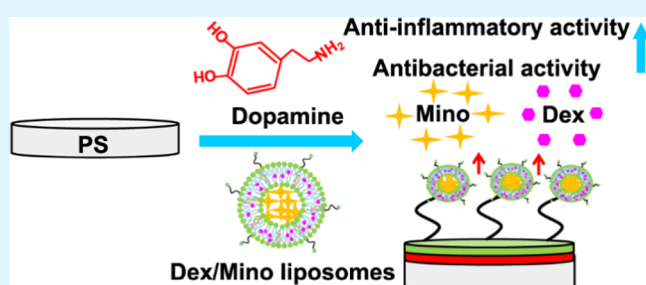
[§]Laboratory of Biomaterials and Regenerative Medicine, Academy for Advanced Interdisciplinary Studies, Peking University, Beijing 100871, P. R. China

^{||}Chongqing Key Laboratory of Oral Diseases and Biomedical Sciences, Chongqing Medical University, Chongqing 401147, P. R. China

Supporting Information

ABSTRACT: Reducing early nonbacterial inflammation induced by implanted materials and infection resulting from bacterial contamination around the implant–abutment interface could greatly decrease implant failure rates, which would be of clinical significance. In this work, we presented a facile and versatile strategy for the construction of anti-inflammatory and antibacterial surfaces. Briefly, the surfaces of polystyrene culture plates were first coated with polydopamine and then decorated with dexamethasone plus minocycline-loaded liposomes (Dex/Mino liposomes), which was validated by contact angle goniometry, quartz crystal microbalance, and fluorescence microscopy. Dex/Mino liposomes were dispersed on functional surfaces and the drug release kinetics exhibited the sustained release of dexamethasone and minocycline. Our results demonstrated that the Dex/Mino liposome-modified surfaces had good biocompatibility. Additionally, liposomal dexamethasone reduced proinflammatory mediator expression (particularly IL-6 and TNF- α) in lipopolysaccharide-stimulated human gingival fibroblasts and human mesenchymal stem cells. Moreover, liposomal minocycline prevented the adhesion and proliferation of *Porphyromonas gingivalis* (Gram-negative bacteria) and *Streptococcus mutans* (Gram-positive bacteria). These findings demonstrate that an anti-inflammatory and antibacterial surface was developed, using dopamine as a medium and combining a liposomal delivery device, which has potential for use to reduce implant failure rates. Accordingly, the surface modification strategy presented could be useful in biofunctionalization of implant materials.

KEYWORDS: liposomes, drug delivery, anti-inflammatory and antibacterial surface, dexamethasone, minocycline, polydopamine



1. INTRODUCTION

Implantable biomedical devices are used broadly when remediless bone loss occurs.¹ The key to successful bone regeneration is proper integration of the surrounding bone with implants, a process referred to as osseointegration.² Nevertheless, because of the influence of early nonbacterial inflammation (caused by surgical trauma, excessive biomechanical stress, or premature prosthetic loading) and bacterial contamination, medical implants frequently suffer from severe postoperative complications, including allergenicity, infection, unsuccessful osseointegration, and loosening, leading ultimately to implant failure.^{3–6} Thus, there is a continuing need to design

anti-inflammatory and antibacterial surfaces on implants to further enhance postoperative success rates. Although some recent studies have focused on preventing early nonbacterial inflammation and bacterial adhesion on implant interfaces,^{7–9} many issues still need to be addressed, including bacterial resistance, excessive drug doses causing systemic side effects, and chemical stability of drug encapsulated in biological materials.

Received: May 5, 2017

Accepted: November 15, 2017

Published: November 15, 2017

An attractive approach to provide reinforced biological properties in implantable devices without sacrificing the advantageous properties of the materials is surface modification. By means of noncovalent or covalent bonding, biochemical immobilization of biomolecules has received particular attention among surface modification methods.^{10,11} Surface immobilization by noncovalent binding could be performed through physical adsorption under particular circumstances. Nevertheless, drawbacks of this approach include the need for comparatively large doses and potentially undesirable biomolecules being released from the implantation site.¹² Conversely, irreversible modification of implant surfaces offers a chance for effective immobilization and orientation of biomolecules with sustained regulation of cell behaviors for extended periods of time.² Surfaces equipped with coatings that have the ability to carry and deliver bioactive molecules to enhance their biological functionality, like preventing device-associated inflammation and infections, are an integral part of this strategy. Nevertheless, it is difficult to deliver bioactive molecules in a controlled manner from a solid substrate surface to decrease risks of implant loosening and failure.

Liposomes are a nanosized, biodegradable, low toxicity, and less immunogenic drug delivery vehicle.¹³ They are widely used as a depot of bioactive agents for controlling drug loading and release in light of their membrane structure.^{14–16} Moreover, local delivery of liposomal drug can keep therapeutic drug levels at a defect site and reduce drug dosage, thus avoiding undesirable side effects correlated with exposure to excessive drug doses. Specifically, liposomal drug delivery is helpful in the treatment of inflammatory diseases,^{17,18} reducing anti-inflammatory drug doses and ultimately the systemic toxicity that commonly results from systemic administration. Additionally, liposomes have been researched broadly as antimicrobial transportation carriers,^{19,20} primarily based on their unique characteristics, such as good biocompatibility, high drug carrying capacity, low occurrence of bacterial resistance, and readily tunable formulation properties. Furthermore, many efforts involving the dual release of bioactive molecules from liposomes have been reported.^{21,22} Previous studies have described that liposomes were (i) covalently immobilized on polystyrene (PS) or metallic surfaces with the aim of biomedical device manufacturing,^{23–27} (ii) covalently bound to an electrospun nanofiber mesh for use in wound dressing applications or bone tissue engineering,^{19,28} (iii) combined with hydrogels for facilitating the development of drug-eluting devices,²⁹ and (iv) assembled with multilayered polymer films providing implantable tissues with better *ex vivo* growth.³⁰ Covalently immobilized liposomes exhibit about a 10-fold increase in time stability when compared with electrostatically bonded liposomes.²⁷ Thus, given this background regarding liposomes, we were motivated to take advantage of these beneficial effects to achieve effective local delivery and controlled dual release of bioactive agents to reduce early nonbacterial inflammation and bacterial contamination. As far as we know, no previous reports have investigated the surface immobilization with liposomes for dual release of active biomolecules on solid implantable devices by chemical covalent conjugation, and for the facilitation of anti-inflammatory and antibacterial activities *in vitro*.

The covalent immobilization of bioactive agent-loaded liposomes, intended to reduce early nonbacterial inflammation and bacterial contamination on the surfaces, is a promising strategy. Here, we describe a multifunctional and versatile

surface modification strategy based on dopamine polymerization. Dopamine molecules can undergo self-polymerization and form extraordinary adhesion on a wide variety of substrate surfaces under weak alkaline conditions without surface pretreatment. In light of Michael addition or Schiff base reactions, a polydopamine (pDA) coating could further couple secondary biopolymers with amines and thiols.^{31,32} To better immobilize liposomes on the surface of a polystyrene (PS) culture plate with a pDA coating, 1,2-distearoyl-*sn*-glycero-3-phosphoethanolamine-*N*-amino (poly(ethylene glycol))-2000 (ammonium salt) (DSPE-PEG-NH₂) molecules were inserted at the surface of drug-loaded liposomes.³³ Then, the modified liposomes were immobilized on the pDA coating via catechol chemistry, wherein the amines of DSPE-PEG-NH₂ could covalently couple to the oxidized catechol groups.³⁴ Minocycline (Mino), a broad-spectrum tetracycline antibiotic, is effective as an antimicrobial agent in periodontal treatment. Also, it is capable of limiting tissue destruction by inhibiting tissue-destroying enzymes, including collagenase, MMP-2, and MMP-9.^{35,36} Dexamethasone (Dex), a potent anti-inflammatory and immunosuppressive glucocorticoid, has been clinically applied to regulate the expression of inflammatory cytokines.^{37,38} Dexamethasone is also noted for promoting osteogenic differentiation as a crucial signaling molecule.³⁹

Guided by these considerations, we first developed and characterized the Dex/Mino liposome-modified PS surfaces in the initial stages. To surface functionalize PS substrates with Dex/Mino liposomes, dopamine was used to bind these two ingredients for the first time. The effects of the Dex/Mino liposome-functionalized surfaces on cell inflammatory response and bacterial adhesion were investigated *in vitro*. For further clinical application, comprehensive fabrication and in-depth investigation of biomolecule-loaded liposome-modified solid implant materials for promoting osteo-differentiation ability are currently underway. The effective and versatile strategy presented here endows the solid substrate with enhanced anti-inflammatory and antibacterial activity, which could ultimately contribute to improving the long-term behavior of the implanted devices. Additionally, this two-step strategy of surface modification shows unique properties, such as availability of simple ingredients, moderate reaction conditions, applicability to numerous kinds of materials, and capacity for multiple applications. We believe that this modification strategy could pave a new way to develop advanced implants targeted at clinical applications.

2. MATERIALS AND METHODS

2.1. Materials. Tris(hydroxymethyl)aminomethane (Tris-HCl) was obtained from Sinopharm Chemical Reagent Co. Ltd. (Beijing, China). Dexamethasone (high-performance liquid chromatography (HPLC), $\geq 98\%$), dopamine hydrochloride, and cholesterol (Chol, Sigma grade, $\geq 99\%$) were provided by Sigma-Aldrich (St. Louis). 1,2-Dipalmitoyl-*sn*-glycero-3-phosphocholine (DPPC) and minocycline hydrochloride were supplied from Tokyo Chemical Industry (TCI, Japan). 1,2-Distearoyl-*sn*-glycero-3-phosphoethanolamine-*N*-amino (poly(ethylene glycol))-2000 (ammonium salt) (DSPE-PEG-NH₂) was obtained from Xi'an ruixi Biological Technology Co. Ltd. (Shanxi, China). *L*- α -Phosphatidylethanolamine-*N*-(lissamine rhodamine B sulfonyl) (ammonium salt) (Egg-Transphosphatidylated, Chicken) (PE-Rho) was bought from Avanti Polar Lipids (Alabaster). Other chemicals were of analytical or HPLC grade. Deionized water (DI water) or phosphate-buffered saline (PBS) was used to prepare all aqueous solutions.

2.2. Formulation and Characterization of Dexamethasone Plus Minocycline-Loaded Liposomes (Dex/Mino Liposomes). A

thin-film hydration method was used to prepare the Dex/Mino liposomes.^{40,41} Briefly, lipids and dexamethasone were dissolved in a chloroform/methanol (1:1, v/v) mixture in a round-bottom flask. A rotary vacuum evaporator was applied to remove methanol and chloroform. Subsequently, the deposited lipids were hydrated in sodium acetate by sonication for 5 min, maintaining the temperature of lipid suspension above the transition temperature ($T_c = 41\text{ }^\circ\text{C}$). Then, dexamethasone liposomes were obtained and subsequently extruded at $T > T_c$ using porous polycarbonate membranes (Millipore, Bedford, MA) with pore sizes of 450, 220, and 100 nm three times, respectively. Unencapsulated sodium acetate was removed by extensive dialysis against physiological saline. Then, an appropriate volume of minocycline hydrochloride solution was mixed with dexamethasone liposomes, incubated at $50\text{ }^\circ\text{C}$ in a water bath, and shaken intermittently for 30 min. Separating liposomes from unencapsulated free drug (minocycline) was carried out by dialysis against PBS at $4\text{ }^\circ\text{C}$.

A Nano Series Zen 4003 Zetasizer (Malvern Instruments Ltd., U.K.) was applied to measure the ζ -potential values, particle sizes, and polydispersity index (PDI). The encapsulation efficiencies (EEs) of dexamethasone and minocycline were determined by the equation: $EE = (W_{\text{encap}}/W_{\text{total}}) \times 100\%$. Here, W_{total} was the measured value of dexamethasone or minocycline in liposome suspensions before dialysis, and W_{encap} was the measured value of dexamethasone or minocycline in liposome suspensions after dialyzing overnight against PBS.

2.3. Preparation and Characterization of Dex/Mino Liposome-Decorated Surfaces. Under weak alkaline ($\text{pH} = 8.5$) conditions, the PS plates were placed into dopamine solution (2 mg/mL in 10 mM Tris-HCl buffer) for 18 h at $37\text{ }^\circ\text{C}$, using a shaker at 70 rpm. Then, the pDA-coated plates were washed with DI water and further immersed in Dex/Mino liposome solution for 24 h. Subsequently, the Dex/Mino liposome-immobilized surfaces were washed gently with PBS.

A contact angle goniometer (SL200B; Kono) was applied to measure water contact angles (WCAs) on the bare and coated PS substrates at ambient temperature. The presence of lipid films on the PS surface was confirmed by X-ray photoelectron spectroscopy (XPS, AXIS Ultra; Kratos Analytical, Ltd., Manchester, U.K.). Field emission scanning electron microscopy (FE-SEM, S-4800; Hitachi Ltd., Tokyo, Japan) was applied to characterize the morphology of the liposome-decorated PS surface, and energy-dispersive spectroscopy (EDS) was applied to differentiate liposomes from pDA particles. All samples were freeze dried and sprayed with gold before observation. The mass variation of the liposome-immobilized PS substrate was evaluated using a quartz crystal microbalance (QCM) (Dongwei Biological Technology Co. Ltd., Hangzhou, China). Binding of PE-Rho-loaded liposomes to the PS substrate was analyzed using fluorescence microscopy and confocal laser scanning microscopy (CLSM; Carl Zeiss, Germany). The semiquantitative average fluorescence intensity of the PE-Rho-loaded liposome-decorated surfaces was determined using a microplate reader (Elx808; Bio-tek).

2.4. In Vitro Release of Dexamethasone and Minocycline. The release profiles of dexamethasone and minocycline from the loaded liposomes without immobilization and immobilized on the PS surface were completed by dialysis against the release medium of PBS. First, 1 mL of the Dex/Mino liposome solution was sealed in the dialysis bags (molecular weight cut-off, 8000–14 000 Da; Union Carbide) and fully immersed in 5 mL of release medium. Also, Dex/Mino liposome-immobilized PS plates were totally immersed in the release medium of PBS. With regard to the release of dexamethasone or minocycline from PS plates without liposomes, PS plates were immersed in a mixed solution of dexamethasone and minocycline similar to their encapsulated concentration in the liposomes in suspension and then immersed into the same release medium. Then, the release medium was maintained at room temperature, followed by shaking at 100 rpm. At a preset time, 0.1 mL of release medium was collected. The content of dexamethasone or minocycline in the release medium at each time point was detected by a high-performance liquid chromatography system (HPLC, Agilent). The UV wavelength of 254

nm was applied to analyze dexamethasone on a C18 column at a flow rate of 1 mL/min. Water, acetonitrile, and phosphoric acid (65:35:0.5, v/v/v) served as the mobile phase. For minocycline, the detection was performed with a 280 nm wavelength at the same flow rate. The mobile phase was composed of 0.2 mol/L ammonium acetate, dimethyl formamide, and tetrahydrofuran (600:398:2, v/v/v), containing 0.01 mol/L disodium ethylenediaminetetraacetic acid.

2.5. In Vitro Cytocompatibility Evaluation.
2.5.1. Cell Culture. Human gingival fibroblasts (HGFs) were isolated from the gingival tissue of a 24 year-old periodontally healthy donor undergoing routine extraction of her third molar teeth with written informed consent. HGFs and human mesenchymal stem cells (hMSCs; ATCC) were cultured in Dulbecco's modified Eagle's medium (DMEM; Gibco) containing 1% (v/v) penicillin (Amresco), 1% (v/v) streptomycin (Amresco), and 10% fetal calf serum (Gibco). The cells were fed every 2–3 days.

2.5.2. Cell Proliferation Assay. The cell counting kit-8 (CCK-8; Dojindo, Japan) was applied to evaluate the proliferation of HGFs and hMSCs, in accordance with the manufacturer's protocol. In brief, HGFs and hMSCs were seeded on 24-well plates with different concentrations (0.5, 1.0, and 2.0 mg/mL) of blank liposomes and Dex/Mino liposome-decorated surfaces at a density of 2.5×10^4 cells/well. The control groups used 10% dimethyl sulfoxide (DMSO) DMEM medium as a positive control and DMEM medium as a negative control. After incubating HGFs for 1, 3, and 5 days and hMSCs for 1, 4, and 7 days, respectively, the medium was aspirated and each sample was rinsed thrice. Then, CCK-8 reagent was transferred to each well with culture medium at a proportion of 1:10 (v/v) in the dark. Supernatant (0.1 mL) was collected to a 96-well plate after a 2 h incubation. A plate reader was used to calculate the optical densities (ODs) at 450 nm.

2.5.3. Cell Morphology Imaging Using Scanning Electron Microscopy (SEM). The morphologies of HGFs or hMSCs cocultured with modified samples were observed using FE-SEM after a 3 day incubation under the culture conditions mentioned above. Briefly, at preset time points, each sample was fixed in glutaraldehyde solution (2.5%, v/v) for 2 h, dehydrated with an ascending ethanol gradient (30–100%, v/v) for 15 min, dried using a vacuum dryer, and sprayed with gold for SEM observation.

2.5.4. Cytoskeletal Observation. After a 3 day incubation, HGFs and hMSCs from each sample were fixed with paraformaldehyde (4%, v/v) for 20 min. Subsequently, Triton X-100 (0.1%, v/v) was used to permeate cells on samples for 5 min, followed by staining cells with fluorescein isothiocyanate (FITC)-phalloidin (5 $\mu\text{g}/\text{mL}$; Sigma) for 30 min. Lastly, samples were immersed in 10 $\mu\text{g}/\text{mL}$ 4',6-diamidino-2-phenylindole (DAPI; Roche, Germany) for 5 min and observed with CLSM.

2.6. In Vitro Anti-Inflammatory Activity Assessment.

2.6.1. Cell Stimulation with Lipopolysaccharide from *Porphyromonas gingivalis* (LPS-PG). HGFs were seeded on pretreated six-well culture plates at a density of 7×10^4 cells/well. After incubating, cells were washed thrice, followed by immersion in serum-free DMEM medium overnight. Then, to create an inflammatory model, the culture medium was replaced with LPS-PG (InvivoGen) solution at 1 $\mu\text{g}/\text{mL}$ in serum-free DMEM, which was incubated in contact with the HGFs for 24 h. Untreated HGFs cultured in serum-free DMEM were used as a control. At a preset time, cells and supernatant were collected and analyzed based on real-time polymerase chain reaction (RT-PCR) and enzyme-linked immunosorbent assay (ELISA), respectively. Also, hMSCs were treated with the same procedure.

2.6.2. RT-PCR. RNA isolation from cells was performed by TRIzol (Invitrogen) treatment, and a Revert Aid First Strand cDNA Synthesis Kit (Thermo) was applied to convert the extracted RNA into cDNA per the manufacturer's protocol. RT-PCR was conducted using SYBR Green (Roche) on an ABI 7500 RT-PCR machine (Applied Biosystems), and β -actin served as a housekeeping gene. The primers used are listed in Table S3. The cycle threshold values (Ct values) were used to determine the fold differences by the $\Delta\Delta\text{Ct}$ method.

2.6.3. ELISA. Proinflammatory cytokine levels were measured in the supernatants from cells with ELISA kits (Beijing Qisong Biological

Table 1. Characterization of the Dex/Mino Liposomes^a

liposomes	particle size (nm)	polydispersity index	ζ potential (mV)	EE (%)	
				Dex	Mino
blank liposomes	154.93 \pm 2.73	0.241 \pm 0.032	-0.78 \pm 0.08		
Dex/Mino liposomes	164.56 \pm 3.04	0.173 \pm 0.017	-2.29 \pm 0.38	11 \pm 0.60	69 \pm 1.30

^aEE, encapsulation efficiency; Dex, dexamethasone; Mino, minocycline; data are presented as mean \pm SD ($n = 3$).

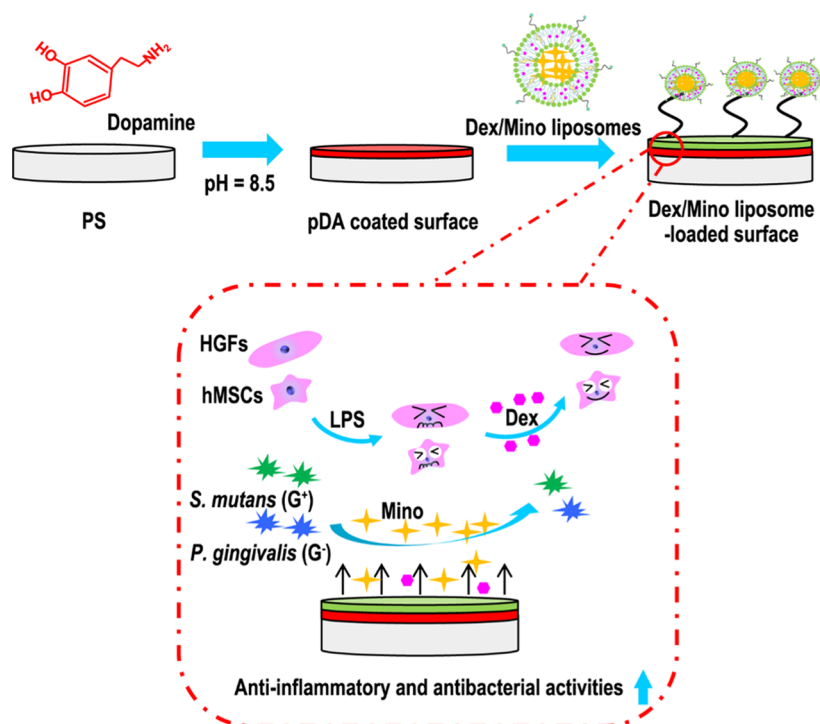


Figure 1. Schematic illustration of the preparation of Dex/Mino liposome-decorated PS substrate through pDA coating as well as its anti-inflammatory and antibacterial activity assays.

Technology Co. Ltd.) per the manufacturer's instruction. Briefly, 50 μ L of the standard solution or 10 μ L of sample with 40 μ L of sample diluent was transferred to the pretreated 96-well plate. Then, horseradish peroxidase-conjugated reagent (0.1 mL) was added and reacted for 1 h at 37 $^{\circ}$ C. Nothing was added to the blank well. After washing five times with washing buffer (1 \times), 3,3',5,5'-tetramethylbenzidine substrate reagent (0.1 mL) was added and reacted at 37 $^{\circ}$ C for 15 min without light. Lastly, the reaction was stopped by adding terminate reagent (50 μ L). An absorbance of 450 nm was used to measure the concentration, and a standard curve generated with standard was used to determine the levels of proinflammatory cytokines in each sample.

2.7. In Vitro Antibacterial Activity Assay. **2.7.1. Bacteria Culture.** Oral bacteria, *P. gingivalis* (ATCC33277, Gram-negative) and *Streptococcus mutans* (UA159, ATCC, Gram-positive), were used in the antibacterial activity assay. *P. gingivalis* were cultured in tryptic soy broth and agar with 1 μ g/mL vitamin K1, 5 μ g/mL hemin, 5 mg/mL yeast extract, and 1:20 (v/v) defibrinated sheep blood. *S. mutans* were cultured in brain heart infusion (BHI; Oxoid) and BHI agar. All samples of *P. gingivalis* were grown under standard anaerobic conditions (80% N₂, 10% H₂, 10% CO₂ at 37 $^{\circ}$ C) for different times. All samples of *S. mutans* were incubated in an aerobic incubator containing 5% CO₂ for the scheduled time at 37 $^{\circ}$ C.

2.7.2. Quantitative Measurement of Bacterial Adhesion and Proliferation. Bacterial adhesion on the surfaces of pristine PS substrates, pDA-modified PS substrates (PS-pDA), 1.0 mg/mL blank liposome-modified PS substrates (PS-1.0 blank lipo), and 1.0 mg/mL Dex/Mino liposome-modified PS substrates (PS-1.0 Dex/Mino lipo) was assessed with the Microbial Viability Assay Kit-WST (Dojindo, Kumamoto, Japan). The control group used culture medium with no

bacteria as a negative control. At scheduled times, substrates were taken out and placed into new 24-well plates, and rinsed gently to remove nonattached bacteria. Then, WST reagent was added to each well with culture medium at a proportion of 1:20 (v/v). After incubating for 2 h without light, supernatant (0.1 mL) was collected to a 96-well plate and a plate reader was employed to calculate the OD value (at $\lambda = 450$ nm) of the suspension in each well. The bacterial suspension (0.1 mL) left in the old 24-well plates was also collected to a new 96-well plate with WST solution (1:20, v/v) followed by measurement.

2.7.3. Morphological Observation by SEM. Prior to observation, glutaraldehyde (2.5%) was used to fix cells on samples for 1 h. Subsequently, all samples were dehydrated with an ascending ethanol gradient (30–100%, v/v) for 15 min, dried in a vacuum dryer, and sprayed with gold.

2.7.4. Live/Dead Fluorescent Staining. CLSM was applied to confirm the amount of bacteria adhered on decorated substrate surfaces. A LIVE/DEAD BacLight bacterial viability kit (L-7007; Invitrogen) was applied to stain the samples in accordance with the manufacturer's instruction, for 15 min in a dark room at 37 $^{\circ}$ C; this was a mixture of SYTO 9 with live bacteria labeling green, and propidium iodide (PI) with dead bacteria appearing red. Then, the stained bacteria were rinsed three times with PBS and observed using CLSM at 10 \times magnification, and the images were taken at $\lambda_{ex} = 488$ nm/ $\lambda_{em} = 543$ nm.

2.8. Statistical Analysis. Data were shown as mean \pm standard deviation (SD). With the help of Origin 8.0 software, statistical analyses were conducted. Significant differences among groups were determined by a one-way analysis of variance plus the Tukey post hoc

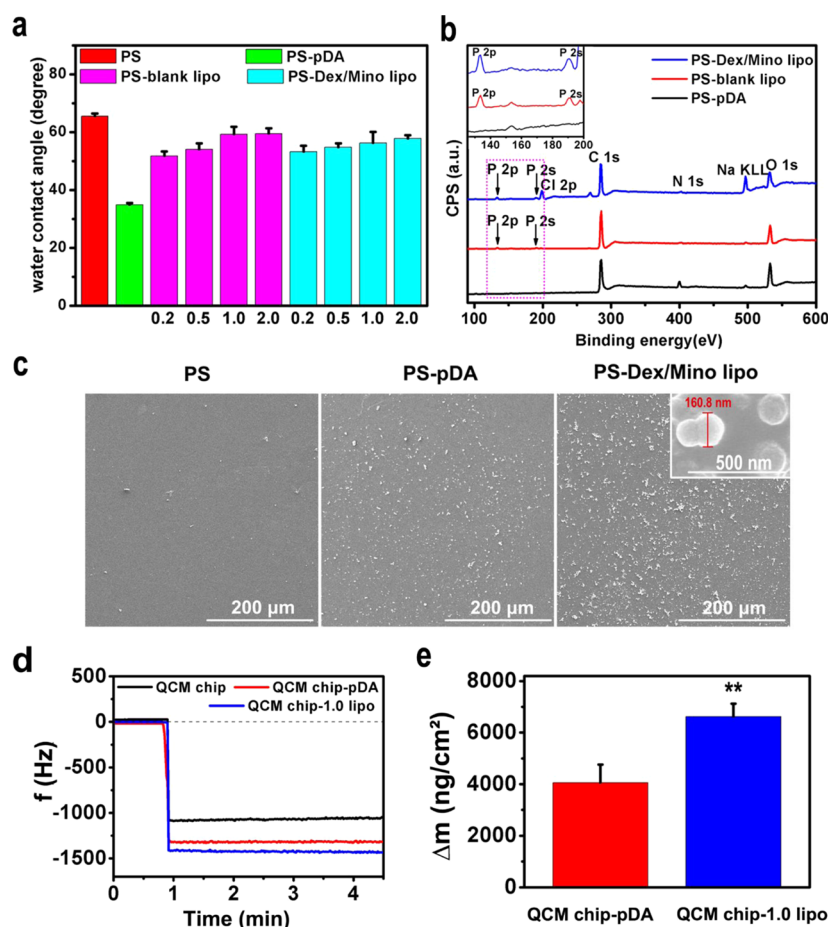


Figure 2. Surface characterization of pristine and functionalized PS substrates. (a) Water contact angle measurements of the modified PS surfaces. In the figure, 0.2, 0.5, 1.0, and 2.0 represent the different concentrations of grafted liposomes (mg/mL). All data represent mean \pm SD ($n = 3$). (b) XPS survey scan spectra. (c) SEM morphology at low (scale bar = 200 μm) and high (scale bar = 500 nm) magnification. (d) Representative frequency change vs time (min) curve. (e) The mass change of QCM chips coated by pDA and liposomes, respectively, and 1.0 represents the concentration of grafted liposomes (1.0 mg/mL). ** $p < 0.01$ compared with chips coated by pDA. All data represent mean \pm SD ($n = 3$).

test. p Values <0.05 and <0.01 indicated statistical significance and high statistical significance, respectively.

3. RESULTS AND DISCUSSION

3.1. Preparation and Characterization of Liposomal Delivery Systems. Liposomes, whose structure and surface properties can be readily majorized, have clear advantages in regulating the delivery of active biomolecules.⁴² Table S1 and Figure S1 present the liposome formulations used in this study. F1, which is composed of cholesterol and DPPC, is defined as a “conventional” liposome. This formulation was applied to optimize the encapsulation efficiency using diverse proportions of dexamethasone and minocycline. F2, which is composed of cholesterol, DPPC, PE-Rho, and DSPE-PEG-NH₂, is known as a “sterically stabilized” liposome. It was applied to detect drug release from liposomes immobilized (DSPE-PEG-NH₂) on functional surfaces. Likewise, this formulation was applied to visualize liposome immobilization by confocal laser scanning microscopy (PE-Rho), and to perform biological assays. Binding to the oxidized catechol groups coated on the PS-pDA surface was facilitated by the DSPE-PEG-NH₂ lipids, forming the outer layer of liposomes. Specifically, the NH₂ groups reacted with oxidized catechol groups at pH 8.5, producing a stable and irreversible link. Moreover, PEGylation

was effective in stabilizing drug-loaded liposomes and averting their aggregation.⁴³

The measured ζ -potential values, particle sizes, and PDI of the liposomes produced with formulation F2 are listed in Tables 1 and S2. The particle sizes of the liposomes exhibited a monodisperse distribution, varying from 154.93 ± 2.73 nm for the blank liposomes to 164.56 ± 3.04 nm for the Dex/Mino liposomes with a low PDI (about 0.2) and nearly neutral ζ -potential values. The encapsulation efficiencies of dexamethasone and minocycline were ~ 11 and $\sim 69\%$, respectively. The sharp difference in encapsulation efficiencies between dexamethasone and minocycline was attributed to the different drug loading methods. The lipophilic drug, dexamethasone, was encapsulated in the liposomes by conventional passive drug loading, whereas the amphipathic weak acid, minocycline hydrochloride, was encapsulated in the liposomes by the efficient active drug loading (acetate gradient) method.^{44–46} Compared with passive liposome encapsulation methods, active loading (also referred to as using transmembrane gradients) leads to a higher drug encapsulation efficiency. It is noteworthy that the driving force for active loading is the pH imbalance.⁴⁵

3.2. Development and Characterization of Dex/Mino Liposome-Decorated Surfaces. Figure 1 illustrates the synthesis process of the Dex/Mino liposome-decorated surfaces with anti-inflammatory and antibacterial activities. Under weak

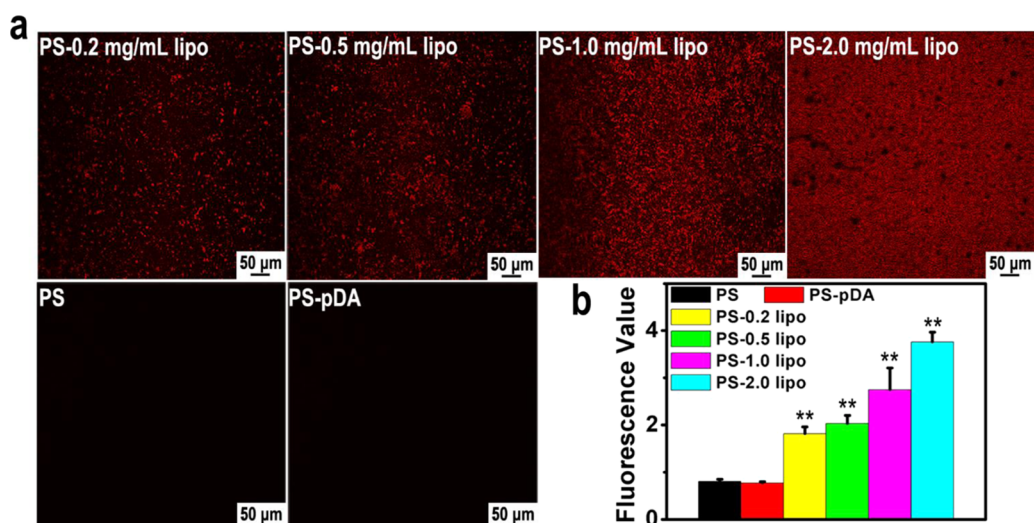


Figure 3. Fluorescently labeled liposomes (PE-Rho liposomes) immobilized onto PS substrates. (a) Fluorescence micrograph of PE-Rho marked liposomes immobilized on the surface of PS substrates. (b) Quantitative grafted-liposome intensity of the liposome-decorated substrates with different concentrations. In the figure, 0.2, 0.5, 1.0, and 2.0 refer to the different concentrations of grafted liposomes (mg/mL). *Statistical significance between the PS group and other grafting groups (** $p < 0.01$). All data represent mean \pm SD ($n = 4$).

alkaline (pH = 8.5) conditions, dopamine molecules could initiate self-polymerization and form a pDA structure,³² which offers plentiful catechol moieties as amine group binders. Dex/Mino liposomes were further grafted to the pDA layer through amine–catechol adduct formation, producing liposome-tethering surfaces. To find any differences in chemical composition and morphology after two stages of surface modification, the Dex/Mino liposome-coated PS surfaces were characterized using contact angle goniometry, XPS, SEM, QCM, and CLSM analyses.

The surface energy and wettability of a substrate can be reflected by the water contact angle (WCA), and contact angle goniometry has been applied widely to assess the availability of surface modification strategy. In this study, the WCA of the various different modified-PS surfaces was assessed by the sessile drop method (Figures 2a and S2). Research has revealed that the hydrophilic properties of biomaterials could be improved by pDA coating.⁴⁷ In line with the earlier literature, the WCA of the pDA-decorated PS surfaces decreased significantly, from 65 ± 2 to $35 \pm 1^\circ$, due to the hydrophilicity of the dopamine molecules with a catecholamine group, indicating that pDA was successfully anchored on the PS surfaces. After the immobilization of blank liposomes at various concentrations (0.2, 0.5, 1.0, and 2.0 mg/mL), the WCA increased to $56 \pm 2^\circ$, and this change in wettability was attributed to successful decoration with liposomes on the pDA-coated PS surfaces. Similarly, when the pDA-coated PS surfaces were decorated with Dex/Mino liposomes at various concentrations (0.2, 0.5, 1.0, and 2.0 mg/mL), the WCA increased to $56 \pm 2^\circ$.

To assess the successful immobilization of lipid films on pDA-coated surfaces, XPS was applied to measure changes in the surface chemistry composition of pDA-coated PS substrates after grafting liposomes. Figure 2b shows the XPS spectra of the modified surfaces. The predominant components of the pDA-coated surfaces were C 1s, N 1s, and O 1s. On attachment of liposomes to the pDA-coated surfaces, the appearance of a phosphorus signal (P 2s and P 2p) indicated successful immobilization of the lipid films on the pDA-coated surfaces. Furthermore, compared with the pDA-modified group and the

blank liposome-modified group, the Dex/Mino liposome-modified group exhibited a distinct increase in sodium and chlorine, because the minocycline hydrochloride was dissolved in PBS. These results clearly indicate that lipid films were immobilized successfully on the pDA-decorated surfaces.

The morphology and surface roughness of PS substrates were altered by pDA coating and pDA-mediated Dex/Mino liposome immobilization. From the SEM images (Figure 2c), it can be seen that the pristine PS sample had a smooth surface morphology compared to that of the modified PS substrates. Many polymerized DA particles were observed on the surface of the pDA-coated PS sample, which had a rough surface morphology compared with that of the bare PS substrate, confirming the pDA layer on the PS surface. Furthermore, the surface roughness/morphology of the PS-pDA substrate was slightly increased by the addition of Dex/Mino liposomes, confirming the preservation of the liposome structure. The inset, an enlarged image of the Dex/Mino liposome-decorated substrate, presents an example of a liposome, sized ~ 160.8 nm, immobilized on the surface of the PS substrate. EDS analysis was also used to assess the characteristic immobilization of liposomes on the surfaces of the PS substrate. Figure S3 reveals the presence of the element phosphorus (P), suggesting that liposome immobilization was successful.

QCM, a sensor system that is generally applied to detect mass change at a sensing surface,⁴⁸ was also used to assess the successful immobilization of liposomes on the pDA-coated surface. Figures 2d,e and S4 show the frequency and mass changes of pDA coating and liposome modification measured by this convincing analytical method. The frequency signals of the pDA-coated surface were notably enhanced, confirming the pDA layer on the QCM chip surface. Furthermore, the addition of liposomes slightly augmented the frequency signals of the pDA-coated surface, confirming the presence of liposomes. Likewise, the mass change of chips decorated by liposomes (6622 ± 506 ng/cm²) was markedly higher than that of the pDA coating (4057 ± 702 ng/cm²) ($p < 0.01$), suggesting the successful decoration of liposomes on the pDA-coated surface.

All results above confirmed that liposomes were conjugated on the modified PS surfaces. Next, it was important to examine

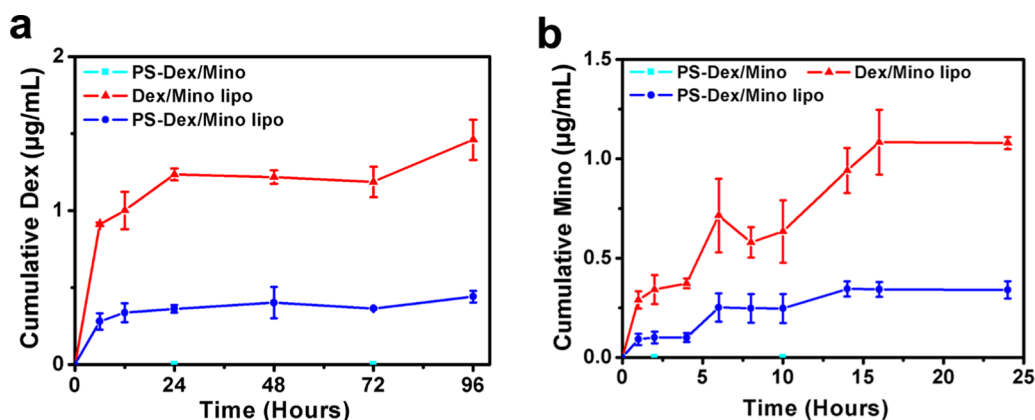


Figure 4. In vitro cumulative release of (a) dexamethasone and (b) minocycline from PS immersed in a mixed solution of dexamethasone and minocycline, and dexamethasone and minocycline release from Dex/Mino liposomes in suspension and immobilized on the surfaces of PS substrates. All data represent mean \pm SD ($n = 3$).

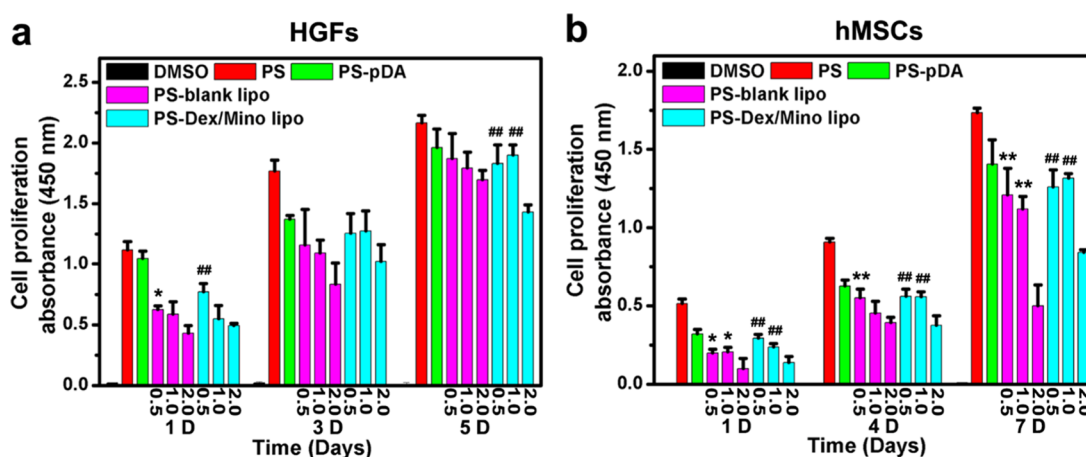


Figure 5. Proliferation of HGFs (a) and hMSCs (b) cultured with different concentrations of liposome-decorated PS. In the figure, 0.5, 1.0, and 2.0 refer to the different concentrations of grafted liposomes (mg/mL). *Statistical significance between 0.5 and 1.0 mg/mL blank liposome groups and 2.0 mg/mL blank liposome group (* $p < 0.05$; ** $p < 0.01$). #Statistical significance between 0.5 and 1.0 mg/mL Dex/Mino liposome groups and 2.0 mg/mL Dex/Mino liposome group (# $p < 0.05$; ## $p < 0.01$). All data represent mean \pm SD ($n = 3$).

whether they were immobilized at the presupposed spatial distribution, for which PE-Rho liposomes were used. Figure 3a presents the representative fluorescence images of the different modified samples, and Figure 3b presents the corresponding semiquantitative analysis. The fluorescence images reveal that the liposomes were dispersed on the surface of the substrates. Moreover, the red fluorescence intensity clearly increased with an increase in the concentration of the grafted PE-Rho liposomes, which is consistent with the semiquantitative results. Conversely, no red signal was observed from the PS or PS-pDA samples that were prepared without decoration and submersion in PE-Rho-loaded liposomes, suggesting the short autofluorescence and lack of immobilization of the liposomes on PS surfaces.

3.3. Drug Release from Liposomes Immobilized on Functional Surfaces. In Figure 4a, the dexamethasone release profile from PS substrates and from liposomes without immobilization and immobilized on the surfaces of decorated PS substrates were followed. The kinetic release profile revealed no release of dexamethasone from the PS group (PS-Dex/Mino). However, the release profile of dexamethasone from liposomes without immobilization (Dex/Mino lipo) was recorded by a sustained release rate for ~ 24 h, followed by a

decreasing release rate during the remaining time. Significantly, a slower but steadier release from liposomes with immobilization was observed in the PS-Dex/Mino lipo group. As suggested previously, the effective concentration of dexamethasone for an anti-inflammatory effect should be within the range of 100–10 000 nM.⁴⁹ The results above are in accordance with the availability of dexamethasone on the surface of liposome-immobilized PS substrates at concentrations appropriate to promote anti-inflammatory activity. Further biological assays were conducted with HGFs and hMSCs to confirm this conclusion.

Likewise, in Figure 4b, the cumulative release profile versus time was followed for minocycline. The kinetic release profile revealed no release of minocycline from the PS group (PS-Dex/Mino). However, the release profile of minocycline from liposomes without immobilization (Dex/Mino lipo) was recorded by a sustained release rate for ~ 14 h, followed by a decreasing release rate during the remaining time. Significantly, a slower but steadier release from liposomes with immobilization was observed in the PS-Dex/Mino lipo group. As shown above, the PS substrates hardly adsorbed free minocycline and no release was also observed in the PS-Dex/Mino group. Nevertheless, better control of minocycline release was

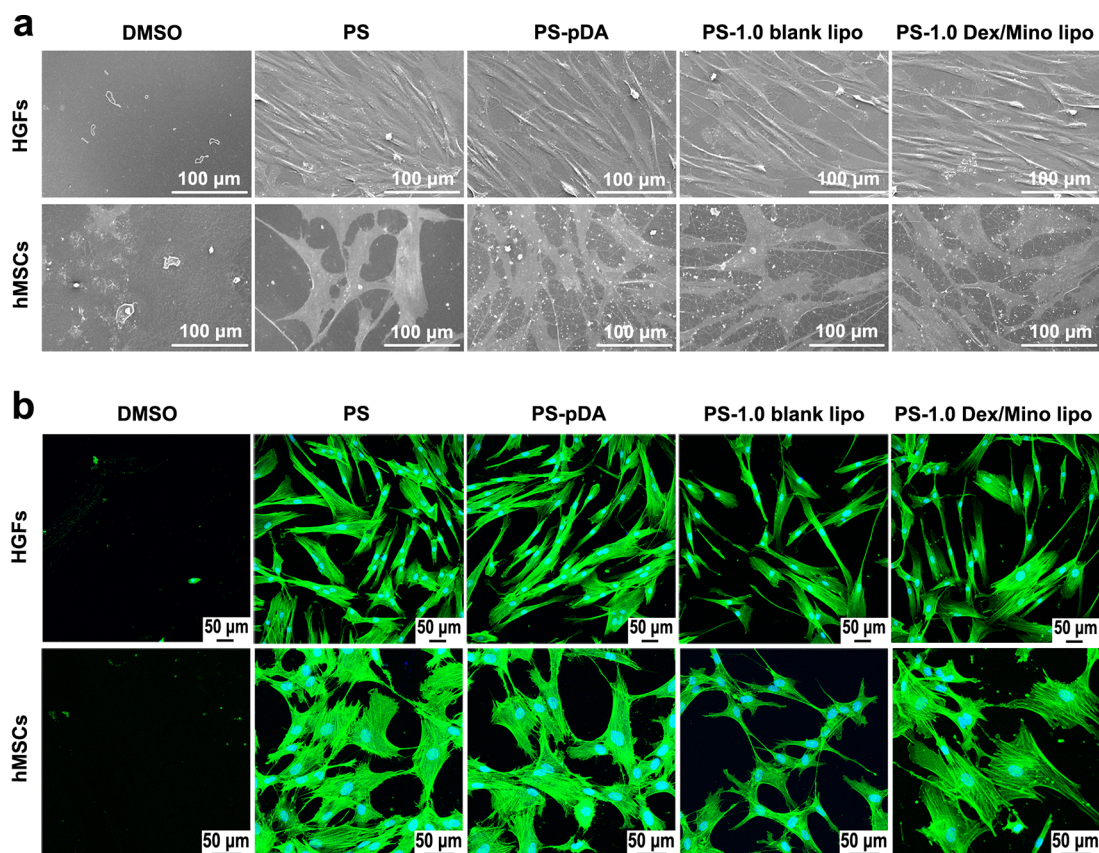


Figure 6. Adherent morphologies of HGFs and hMSCs after incubation with pristine and decorated PS substrates for 3 days. (a) SEM images; (b) CLSM images of adherent morphology and actin cytoskeletal organization (green, labeled with FITC-phalloidin, counterstained with DAPI for nuclei in blue). In the figure, 1.0 represents the concentration of grafted liposomes (1.0 mg/mL).

observed when the liposomes were immobilized on the surface of the PS substrate. In this regard, we could draw the conclusion that the minocycline release was controlled by the liposome structure.

3.4. In Vitro Cytocompatibility Evaluation. The cytocompatibility of the liposome-modified surfaces for HGFs and hMSCs is another important factor that should be assessed if the novel liposome-decorated materials are to be used in implant application. Figure 5a,b, respectively, present the in vitro HGF and hMSC proliferation capacities when cultured with pristine and various concentrations (0.5, 1.0, and 2.0 mg/mL) of liposome-decorated PS samples in DMEM for 1, 3 (4), and 5 (7) days, evaluated by CCK-8 assays, revealing that all test groups showed good time-dependent cell growth. The OD_{450} values increased with time, suggesting that the liposome-decorated surfaces had good cytocompatibility and could also facilitate normal proliferation of HGFs and hMSCs. However, in contrast with the PS control, lower OD_{450} values were detected in all experimental groups during incubations ($p < 0.05$), implying somewhat negative influences of the liposome-decorated surfaces on cell growth. A reasonable interpretation is that the hydrophobicity and PEGylated coating of liposomes used for the drug delivery system might inhibit initial cell adhesion to some extent. However, the 0.5 and 1.0 mg/mL Dex/Mino lipo groups and the 0.5 and 1.0 mg/mL blank lipo groups exhibited higher OD_{450} values than those of the 2.0 mg/mL Dex/Mino lipo group and the 2.0 mg/mL blank lipo group ($p < 0.05$) after incubating HGFs for 1 and 5 days and incubating hMSCs for 1, 4, and 7 days, respectively, although

no statistically significant differences were observed between the 0.5 and 1.0 mg/mL Dex/Mino lipo groups or between the 0.5 and 1.0 mg/mL blank lipo groups ($p > 0.05$) during the culture periods. These findings suggest that the concentration of grafted liposomes could affect the in vitro cytocompatibility of the samples, and 1.0 mg/mL of liposome-decorated surface could greatly facilitate the proliferation of HGFs and hMSCs. On the basis of our results, 1.0 mg/mL may be the most appropriate concentration of liposomes for decorating PS substrates to steer cellular fates.

To further investigate the cytocompatibility of the modified surfaces, we examined the adherent morphologies of the HGFs and hMSCs. Figure 6 presents a typical overview of the HGF and hMSC morphologies growing with different decorated PS substrates for 3 days. The SEM images in Figure 6a reveal that HGFs and hMSCs cultured on all samples had healthy shapes. However, compared with those of the blank liposome-decorated group, cells with moderately better adhesion and spreading were seen in the Dex/Mino liposome-decorated group. Similarly, the fluorescence images (Figure 6b) show that HGFs and hMSCs exhibited narrow spreading and filamentous morphology on the blank liposome-decorated surfaces, and F-actin was poorly developed. However, in the Dex/Mino liposome-decorated group, HGFs and hMSCs attached and spread more than those in the blank liposome-decorated group. A possible explanation is that the blank liposomes on the PS substrates might initiate a mild inflammatory response in the HGFs and hMSCs, but the Dex/Mino liposome-decorated surfaces mitigated the foreign body response by slow release of

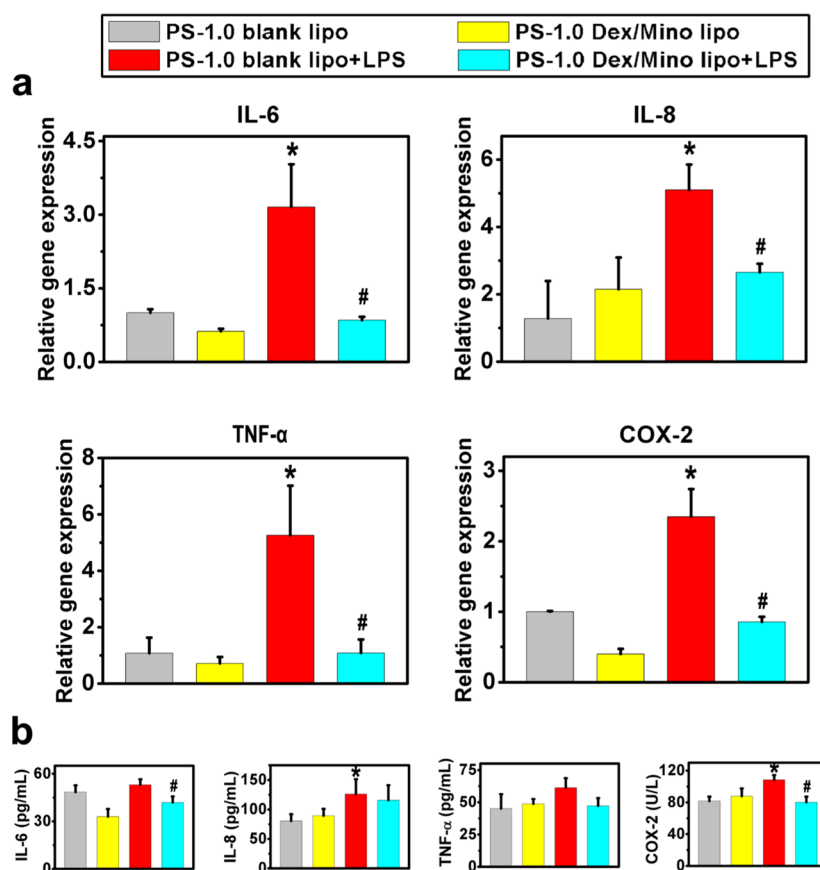


Figure 7. Anti-inflammatory activity of Dex/Mino liposome-functionalized PS samples against HGFs cultured with LPS for 24 h. (a) RT-qPCR analysis: effects of Dex/Mino liposomes on LPS-induced IL-6, IL-8, TNF- α , and COX-2 expression levels in HGFs. (b) ELISA analysis: effects of Dex/Mino liposomes on LPS-induced IL-6, IL-8, TNF- α , and COX-2 protein levels in HGFs. In the figure, 1.0 refers to the concentration of grafted liposomes (1.0 mg/mL). *#Statistical significance between the PS-1.0 blank liposome group and PS-1.0 blank liposomes + LPS group, and the PS-1.0 blank liposomes + LPS group and PS-1.0 Dex/Mino liposomes + LPS group, respectively (*# $p < 0.05$). All data represent mean \pm SD ($n = 3$).

dexamethasone, a celebrated anti-inflammatory drug with power to mitigate foreign body response at an implant site.⁵⁰ Our results indicate that surface immobilization of Dex/Mino liposomes might facilitate the adhesion and spreading of HGFs and hMSCs on pDA-decorated substrates. Furthermore, compared with cells in the blank liposome-decorated group, HGFs and hMSCs cultured with the Dex/Mino liposome-decorated group and the pristine PS group spread more adherent filopodia and extended more mature F-actin intracellular stress fibers, implying that Dex/Mino liposomes had a positive effect on cell growth, and appropriate surface modification with Dex/Mino liposomes could endow the substrates with more desirable cytocompatibility.

3.5. In Vitro Anti-Inflammatory Activity Assay.

Destructive inflammatory mediators induced during an inflammatory response were reported to inhibit osteoblast function and promote osteoclastic activity, and also to perpetuate inflammation.⁵¹ Chemokines, such as IL-8, are important chemoattractants that recruit neutrophils to injured lesions. Matrix metalloproteinases can be released from neutrophils and then tissue injury ensues.⁵² IL-6, a multifunctional cytokine, has potential for activation of osteoclasts and inducing bone resorption.⁵² TNF- α is a well-known proinflammatory cytokine, triggering a cascade of events resulting in further release of other inflammatory mediators, such as cyclooxygenase type 2 (COX-2), a key inducible enzyme stimulating and amplifying inflammation.^{18,53,54} These proin-

flammatory mediators that cause local and systemic inflammation may result in damage to injured tissue, thus accelerating the eventual failure of many implanted medical devices. As mentioned above, dexamethasone is a potent anti-inflammatory drug that is used widely in various biomaterials strategies to mitigate inflammatory responses.^{39,55,56} Under the condition of inflammatory stimulus, dexamethasone exerts its anti-inflammatory effects largely by modulating the synthesis and release of inflammatory mediators.⁵⁷ In our study, the Dex/Mino liposome-modified surfaces exhibited potential for use as a modification strategy, with the controlled release of dexamethasone at a localized site due to its retention in the liposome structure. Thus, we further investigated whether dexamethasone released from the Dex/Mino liposome-modified surfaces was active, and whether the amount of dexamethasone released from the Dex/Mino liposome-modified surfaces would be sufficient to mitigate the inflammatory response to LPS.

Gene expression analyses from HGFs cultured on different surfaces, using RT-PCR, revealed that Dex/Mino liposome-modified surfaces effectively inhibited the expression of proinflammatory mediators (such as IL-6, IL-8, TNF- α , and COX-2) stimulated by LPS. Figure 7a shows the relative gene expression at 24 h. At a preset time, the HGFs cultured with LPS on blank liposome-decorated surfaces exhibited higher mRNA expression of IL-6, IL-8, TNF- α , and COX-2. However, the slow release of dexamethasone effectively downregulated

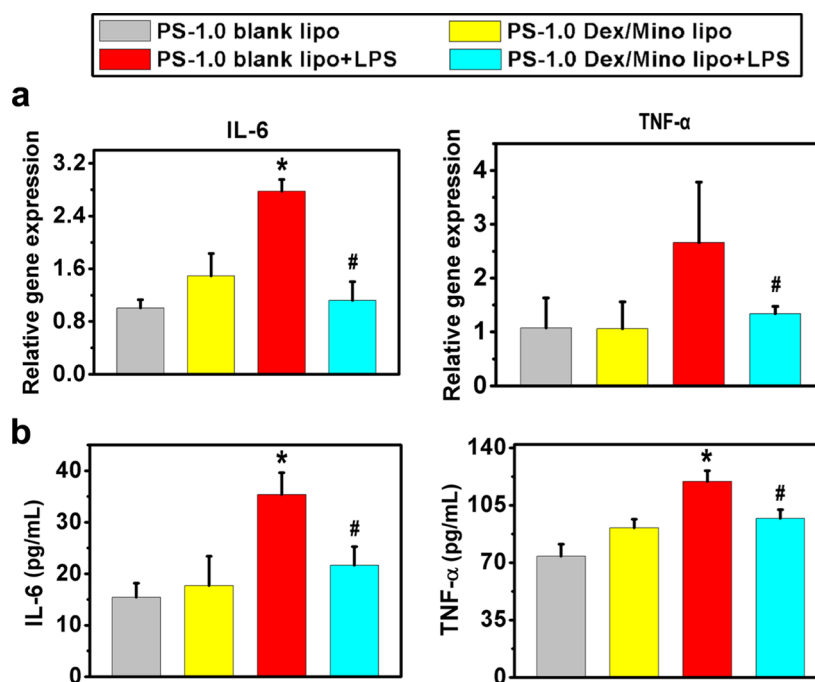


Figure 8. Anti-inflammatory activity of Dex/Mino liposome-functionalized PS samples against hMSCs cultured with LPS for 24 h. (a) RT-qPCR analysis: effects of Dex/Mino liposomes on LPS-induced IL-6 and TNF- α expression levels in hMSCs. (b) ELISA analysis: effects of Dex/Mino liposomes on LPS-induced IL-6 and TNF- α protein levels in hMSCs. In the figure, 1.0 refers to the concentration of grafted liposomes (1.0 mg/mL). *#Statistical significance between the PS-1.0 blank liposome group and PS-1.0 blank liposomes + LPS group, and the PS-1.0 blank liposomes + LPS group and PS-1.0 Dex/Mino liposomes + LPS group, respectively (*# $p < 0.05$). All data represent mean \pm SD ($n = 3$).

the expression of proinflammatory mediators at the mRNA level in HGFs cultured with LPS on Dex/Mino liposome-decorated surfaces. To confirm the anti-inflammatory activity of dexamethasone, its inhibitory action on LPS-induced IL-6, IL-8, TNF- α , and COX-2 expression at 24 h was assessed using ELISA (Figure 7b). The difference in protein expression between pristine and Dex/Mino liposome-decorated PS substrates was consistent with the RT-PCR results. Additionally, treatment with dexamethasone alone had little effect on IL-6, IL-8, TNF- α , or COX-2 at the mRNA and protein levels, in contrast with the control group. These results indicate that LPS markedly upregulated the expression of IL-6, IL-8, TNF- α , and COX-2 at both the mRNA and protein levels. However, dexamethasone released from Dex/Mino liposome-decorated surfaces effectively repressed LPS-induced expression of proinflammatory mediators at both the mRNA and protein levels. Given these results, Dex/Mino liposomes could be useful components for immobilization on pDA-coated substrates designed to function in an anti-inflammatory manner.

We also investigated gene expression in hMSCs cultured on different surfaces using quantitative RT-PCR. Figure 8a shows that Dex/Mino liposome-modified surfaces effectively inhibited the expression of proinflammatory mediators, such as IL-6 and TNF- α , when stimulated with LPS for 24 h. Over a scheduled culture period, hMSCs stimulated with LPS on blank liposome-decorated surfaces exhibited much higher mRNA levels of IL-6 and moderately higher mRNA levels of TNF- α . However, hMSCs cultured with LPS on Dex/Mino liposome-decorated surfaces exhibited effectively downregulated IL-6 and TNF- α mRNA levels, because of the slow release of dexamethasone. We performed ELISA assays to detect the anti-inflammatory activity of dexamethasone on LPS-induced IL-6 and TNF- α secretion in hMSCs. Figure 8b shows that hMSCs induced by

LPS exhibited markedly increased protein expression of IL-6 and TNF- α , but hMSCs cultured with LPS on Dex/Mino liposome-decorated surfaces exhibited effective downregulation in IL-6 and TNF- α secretion, which is consistent with the RT-PCR results. These results indicate that dexamethasone released from Dex/Mino liposome-decorated surfaces effectively suppressed LPS-induced IL-6 and TNF- α expression at the mRNA and protein levels, in contrast with the LPS group.

Taken together, our study described above indicates that the encapsulation process through dual-loaded liposomes did not change the structure or function of dexamethasone, and so presumably still allows the effective combination of dexamethasone with its receptor. Furthermore, although only $\sim 11\%$ of dexamethasone was encapsulated in the Dex/Mino liposome-decorated surfaces, it was sufficient and active to exert anti-inflammatory effects. Overall, the observed anti-inflammatory effectiveness of locally released dexamethasone implies that the strategy for Dex/Mino liposome-decorated surfaces has potential clinical applications for implant surface modification.

3.6. In Vitro Antibacterial Activity Analysis. A pivotal step in biofilm formation as well as an essential part of the pathogenesis of infection is the initial adhesion of bacteria to implant interfaces.⁵⁸ In the early stage of postimplantation, it is key to prevent bacterial adhesion onto implanted biomaterials, to increase the efficacy and maintain the sustained success of implants. In our study, both *P. gingivalis* (Gram-negative), one of the most common bacteria in peri-implantitis and periodontitis,⁵⁹ and *S. mutans* (Gram-positive), the major pathogenic microbe of dental caries and one of the early colonizers in dental plaque biofilm,⁶⁰ were used to assess bacterial attachment on the Dex/Mino liposome-modified surfaces. To reveal the antibacterial effects of the coated surfaces, we assessed the quantities, morphologies, and

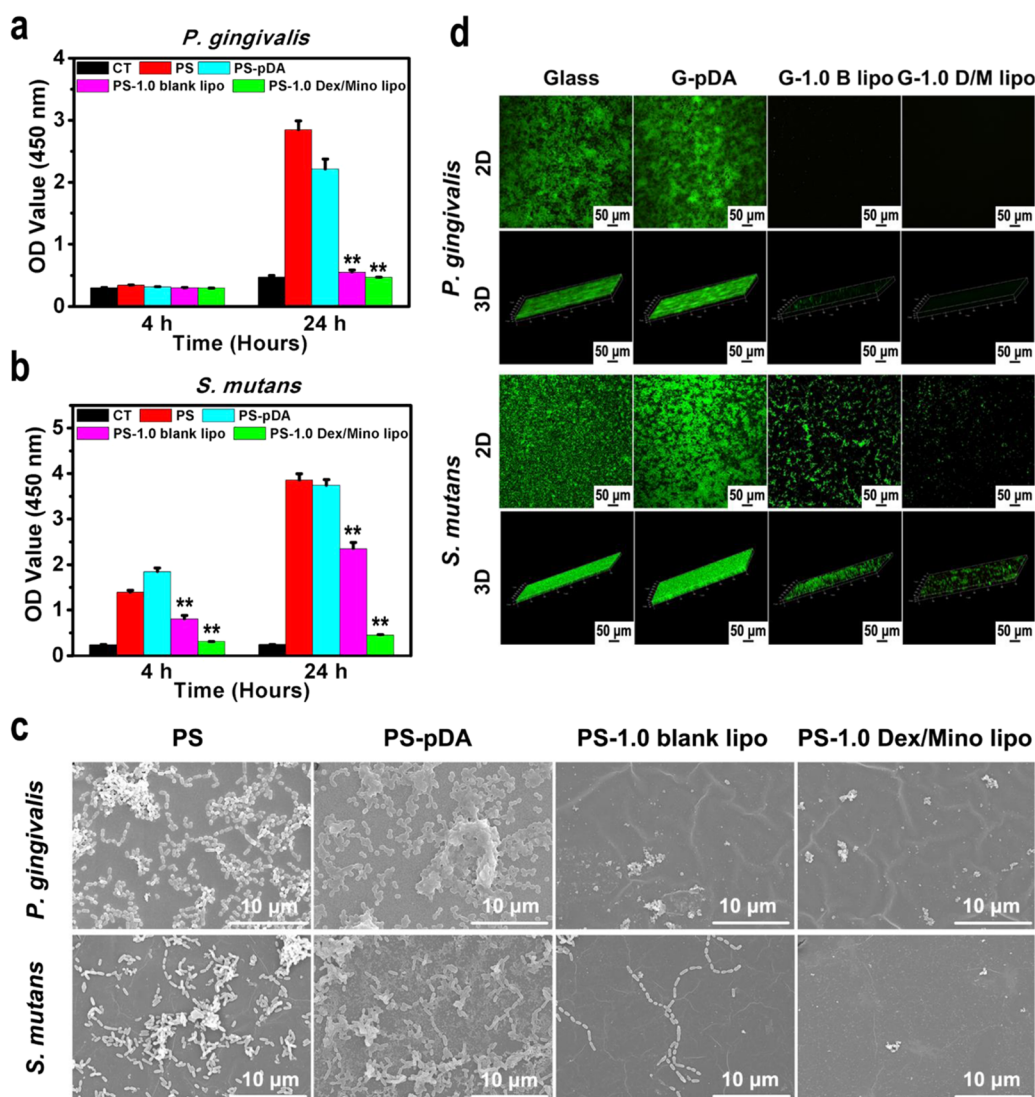


Figure 9. Antibacterial activity of pristine and functionalized PS samples against (a) Gram-negative *P. gingivalis* and (b) Gram-positive *S. mutans* cultured for 4 and 24 h. *Statistical significance level between the PS group and PS-1.0 blank liposome group or the PS-1.0 Dex/Mino liposome group (** $p < 0.01$). All data represent mean \pm SD ($n = 3$). (c) SEM images of morphology and amounts of *P. gingivalis* and *S. mutans* adhered after a 24 h incubation with pristine and functionalized PS surfaces. (d) Live/dead cell staining on the pristine and functionalized PS surfaces after a 24 h incubation with *P. gingivalis* and *S. mutans*. In the figure, 1.0 refers to the concentration of grafted liposomes (1.0 mg/mL).

viabilities of bacteria adhered on the surface after incubation for a scheduled time.

The viable bacteria on different surfaces were quantified using microbial viability assay kits (Figure 9a,b), which revealed the amount and viability of *P. gingivalis* and *S. mutans* that adhered on the bare PS, PS-pDA, and PS-liposome surfaces. At the initial adhesion stage (4 h), fewer *S. mutans* were detected on the Dex/Mino liposome-modified surfaces compared with that of the bare PS group, indicating the effective antibacterial properties of the Dex/Mino liposome-modified substrates. In the proliferation phase (24 h), the OD values of both *P. gingivalis* and *S. mutans* cultured on the bare PS surfaces increased with time, implying that bare PS substrates were prone to bacterial proliferation. Nevertheless, a decrease in the amount of both adherent bacteria on the Dex/Mino liposome-decorated surfaces was detected. Specifically, after 24 h of incubation with *P. gingivalis*, the Dex/Mino liposome-decorated group exhibited >98% decrease in bacterial adhesion versus that of the bare PS group. For *S. mutans*, the

Dex/Mino liposome-decorated group exhibited similar efficacy (~92%) in reducing the amount of adherent bacteria. Hydrophilic surfaces are commonly considered to have effective resistance to bacteria,⁷ which is consistent with these findings. On the blank liposome-decorated surfaces, the amount of adhered bacteria was notably reduced compared with that on the bare PS surfaces. As shown in Figures 9a and S5a, at 24 h of contact with *P. gingivalis*, the blank liposome-decorated substrate had >98% reduction in bacterial adhesion versus that of the pristine PS group, which exhibited no significant difference compared with that of the Dex/Mino liposome-decorated group. However, suspensions of the blank liposome-decorated group had 1.3-fold more bacterial cells compared to that the pristine PS group, and suspensions of the Dex/Mino liposome-decorated group still had low levels of bacteria (similar to the control). Similar results were obtained for *S. mutans* (Figures 9b and S5b). These findings indicate that liposome-decorated surfaces can effectively inhibit bacterial adhesion, to some extent, and that minocycline released in the

Dex/Mino liposome-decorated group could further inhibit and kill the bacteria.

SEM was used to view the morphology and amount of bacteria incubated for 24 h on pristine PS and the modified surfaces. As shown in Figure 9c, *P. gingivalis* displayed ellipsoid or short-rod morphologies, whereas *S. mutans* displayed short-chain or coccal forms. Many bacteria were found on the bare PS and the pDA-coated surfaces for both *P. gingivalis* and *S. mutans* after 24 h of culture. In contrast, few bacteria appeared on the blank liposome-decorated surfaces and almost no bacteria were found on the Dex/Mino liposome-decorated surfaces, which is similar to the results of the quantitative determination. SEM revealed fewer adhered bacteria on the Dex/Mino liposome-decorated samples than on the pristine ones, demonstrating the efficacy of the Dex/Mino liposome-decorated substrates. The results suggest that minocycline retained its activity after being loaded into the liposomes, followed by immobilization on the pDA-decorated surfaces.

Over the same time period (24 h), we performed bacterial live/dead fluorescent staining assay and used CLSM to identify the status of the bacteria. As shown in Figure 9d, large amounts of bacteria (both *P. gingivalis* and *S. mutans*) were alive on the bare PS and pDA-coated surfaces, along with dense biofilm formation. However, few *S. mutans* were observed on the blank liposome-decorated surfaces and only a small amount of *S. mutans* were found on the Dex/Mino liposome-decorated surfaces. Furthermore, almost no *P. gingivalis* and no trace of biofilm were observed on the blank liposome-modified surfaces and Dex/Mino liposome-decorated surfaces, which is consistent with the corresponding quantification and SEM analysis, suggesting that the liposomal modification and the minocycline released from the Dex/Mino liposome-decorated surfaces contributed to inhibiting bacterial adhesion and proliferation. In addition, it is good to be reminded that dead bacteria might be found on the surface because of natural apoptosis during the bacteria growth process.^{61,62} In Figure 9d, we found a small amount of dead bacteria labeled red in the single channel (PI, 543 nm). Also, we found a large amount of live bacteria labeled green in the single channel (SYTO 9, 488 nm). However, when we combined the two channels together, we hardly observed the labeled red. This may be because the strong green fluorescence signal covered the weak red fluorescence signal.

Minocycline, the semisynthetic derivative of tetracycline, is used clinically in the mechanical treatment of peri-implantitis lesions as an adjuvant.⁶³ In light of its fibroblast-stimulating, antibacterial, and anticollagenase properties, minocycline is also used in bone grafting.⁶⁴ It is well established that the antimicrobial mechanism of minocycline is based on binding to a specific ribosomal subunit, turning off the combination of aminoacyl-tRNA with bacterial ribosome. The suppression hinders the synthesis of bacterial peptides and ribosomal proteins, resulting in bacterial cell death.^{65,66} Covalent immobilization of biomolecules at the surface of different biomedical devices has attracted great interest because it leads to strong and stable attachment. Antibacterial agents directly immobilized on the implant interface by chemical covalent conjugation will not be released readily, limiting the application of biocompatible antibacterial agents (such as minocycline) acting inside the cell. However, a liposomal delivery system covalently bonded to the surface, which could then deliver and slowly release loaded drug, appears promising. Moreover, the distinct bilayer structure of liposomes could fuse with bacterial membranes and release their contents into the cytoplasm.⁴²

Thus, our innovative strategy of using Dex/Mino liposomes immobilized by a mussel-inspired pDA coating may provide enhanced antibacterial activity to the decorated substrates, which would be of importance in preventing implant-associated infections.

4. CONCLUSIONS

Overall, we synthesized Dex/Mino liposomes and developed a Dex/Mino liposome-modified surface with enhanced anti-inflammatory and antibacterial activities that was prepared via catechol chemistry, coating of dopamine on the PS surface, followed by the bonding of Dex/Mino liposomes. Static contact angle, QCM, and fluorescence microscopy confirmed that Dex/Mino liposomes were successfully grafted onto the pDA-coated surfaces. The encapsulation efficiency indicated that the liposomes had outstanding loading capacity. Furthermore, the drug release curves revealed the sustained release of dexamethasone and minocycline, which could provide sufficient dexamethasone and minocycline concentrations for reducing nonbacterial inflammation and bacterial contamination in vitro. After a 7 day incubation, the Dex/Mino liposome-modified surfaces exerted a positive influence on in vitro cell proliferation, spreading, and morphology with HGFs and hMSCs, particularly at a concentration of 1 mg/mL, which indicates that the Dex/Mino liposome-modified surfaces have good biocompatibility. Importantly, the Dex/Mino liposome functionalization of substrates could further reduce proinflammatory cytokine secretion in LPS-stimulated HGFs and hMSCs, confirming that dexamethasone released from the liposome-modified surfaces could preserve its biological activity and effectively decrease nonbacterial inflammation in HGFs and hMSCs induced by LPS. Furthermore, after a 24 h incubation, the Dex/Mino liposome-modified surfaces exhibited effective inhibitory action toward Gram-negative *P. gingivalis* and Gram-positive *S. mutans*. These findings suggest that Dex/Mino liposome-modified surfaces may have value in improving the anti-inflammatory and antibacterial efficacies of various matrix materials, and provide prospects for prolonging the long-term success of various implants. Future work will include the modification of bioactive factor-loaded liposomes on implantable materials for enhanced osteogenesis in vitro and the transplantation of liposome-decorated material in vivo to study osseointegration. In conclusion, we demonstrated a material modification strategy using liposomes immobilized on a pDA-coating surface for use with medical devices for the local and sustained release of bioactive agents relevant for advanced implant applications.

■ ASSOCIATED CONTENT

Supporting Information

The Supporting Information is available free of charge on the ACS Publications website at DOI: 10.1021/acsami.7b06295.

Liposome formulations; representative images of water droplet on the modified PS surfaces; EDS spectrum of Dex/Mino liposome-modified surface; the frequency and mass change of pDA coating and liposome modification; antibacterial activity tests of pristine and functionalized PS samples against *P. gingivalis* and *S. mutans* bacteria cultured in suspension; characterization of liposomes; primer sequences used for RT-PCR analysis (PDF)

AUTHOR INFORMATION

Corresponding Authors

*E-mail: wx13121709448@163.com. Phone/Fax: +86 10 83911069 (L.W.).

*E-mail: sc-wei@pku.edu.cn. Phone/Fax: +86 10 82195780 (S.W.).

ORCID

Shicheng Wei: 0000-0001-5570-3393

Author Contributions

Each author listed on this manuscript was involved in completing the manuscript and agreed to the final manuscript.

Notes

The authors declare no competing financial interest.

ACKNOWLEDGMENTS

Support for this work was afforded by the National Natural Science Foundation of China (No. 81571814), China Railway China Science and Technology Research and Development Project (No. J2015C001-J), Chongqing Research Program of Basic Research and Frontier Technology (No. cstc2016jcyjA0199), and Science and technology project of Yubei District in Chongqing (No. 2017-36). We thank Lei Liu and Wenbin Dai (School of Pharmaceutical Sciences, Peking University) for their assistance in liposome preparation and measurement. We thank Professor Jianguo Ji, Qingsong Wang, Hui Li, and Gaojun Liu (School of Life Sciences, Peking University) for their help with HPLC measurement. We also thank Fei He and Ping Zhou for their help in QCM measurement.

REFERENCES

(1) Navarro, M.; Michiardi, A.; Castaño, O.; Planell, J. A. *Biomaterials in Orthopaedics. J. R. Soc., Interface* **2008**, *5*, 1137–1158.

(2) Xu, A.; Zhou, L.; Deng, Y.; Chen, X.; Xiong, X.; Deng, F.; Wei, S. A Carboxymethyl Chitosan and Peptide-Decorated Polyetheretherketone Ternary Biocomposite with Enhanced Antibacterial Activity and Osseointegration as Orthopedic/Dental Implants. *J. Mater. Chem. B* **2016**, *4*, 1878–1890.

(3) Winnett, B.; Tenenbaum, H. C.; Ganss, B.; Jokstad, A. Perioperative Use of Non-Steroidal Anti-Inflammatory Drugs Might Impair Dental Implant Osseointegration. *Clin. Oral Implants Res.* **2016**, *27*, e1–e7.

(4) Deng, Y.; Zhou, P.; Liu, X.; Wang, L.; Xiong, X.; Tang, Z.; Wei, J.; Wei, S. Preparation, Characterization, Cellular Response and *in Vivo* Osseointegration of Polyetheretherketone/Nano-Hydroxyapatite/Carbon Fiber Ternary Biocomposite. *Colloids Surf., B* **2015**, *136*, 64–73.

(5) Wang, L.; He, S.; Wu, X.; Liang, S.; Mu, Z.; Wei, J.; Deng, F.; Deng, Y.; Wei, S. Polyetheretherketone/Nano-Fluorohydroxyapatite Composite with Antimicrobial Activity and Osseointegration Properties. *Biomaterials* **2014**, *35*, 6758–6775.

(6) Mouhyi, J.; Ehrenfest, D. M. D.; Albrektsson, T. The Peri-Implantitis: Implant Surfaces, Microstructure, and Physicochemical Aspects. *Clin. Implant Dent. Relat. Res.* **2012**, *14*, 170–183.

(7) Wu, H.-X.; Tan, L.; Tang, Z.-W.; Yang, M.-Y.; Xiao, J.-Y.; Liu, C.-J.; Zhuo, R.-X. Highly Efficient Antibacterial Surface Grafted with a Triclosan-Decorated Poly(N-Hydroxyethylacrylamide) Brush. *ACS Appl. Mater. Interfaces* **2015**, *7*, 7008–7015.

(8) Rubert, M.; Li, Y.-F.; Dehli, J.; Taskin, M. B.; Besenbacher, F.; Chen, M. Dexamethasone Encapsulated Coaxial Electrospun PCL/PEO Hollow Microfibers for Inflammation Regulation. *RSC Adv.* **2014**, *4*, 51537–51543.

(9) Qin, H.; Cao, H.; Zhao, Y.; Zhu, C.; Cheng, T.; Wang, Q.; Peng, X.; Cheng, M.; Wang, J.; Jin, G.; Jiang, Y.; Zhang, X.; Liu, X.; Chu, P. K. *In Vitro* and *In Vivo* Anti-Biofilm Effects of Silver Nanoparticles Immobilized on Titanium. *Biomaterials* **2014**, *35*, 9114–9125.

(10) Zheng, D.; Neoh, K. G.; Shi, Z.; Kang, E.-T. Assessment of Stability of Surface Anchors for Antibacterial Coatings and Immobilized Growth Factors on Titanium. *J. Colloid Interface Sci.* **2013**, *406*, 238–246.

(11) de Jonge, L. T.; Leeuwenburgh, S. C. G.; Wolke, J. G. C.; Jansen, J. A. Organic–Inorganic Surface Modifications for Titanium Implant Surfaces. *Pharm. Res.* **2008**, *25*, 2357–2369.

(12) Morra, M. Biochemical Modification of Titanium Surfaces: Peptides and ECM Proteins. *Eur. Cells Mater.* **2006**, *12*, 1–15.

(13) Hallaj-Nezhadi, S.; Hassan, M. Nanoliposome-Based Antibacterial Drug Delivery. *Drug Delivery* **2015**, *22*, 581–589.

(14) Ju, R.-J.; Li, X.-T.; Shi, J.-F.; Li, X.-Y.; Sun, M.-G.; Zeng, F.; Zhou, J.; Liu, L.; Zhang, C.-X.; Zhao, W.-Y.; Lu, W.-L. Liposomes, Modified with PTDHIV-1 Peptide, Containing Epirubicin and Celecoxib, to Target Vasculogenic Mimicry Channels in Invasive Breast Cancer. *Biomaterials* **2014**, *35*, 7610–7621.

(15) Allen, T. M.; Cullis, P. R. Liposomal Drug Delivery Systems: From Concept to Clinical Applications. *Adv. Drug Delivery Rev.* **2013**, *65*, 36–48.

(16) Liu, Y.; Lu, W.-L.; Guo, J.; Du, J.; Li, T.; Wu, J.-W.; Wang, G.-L.; Wang, J.-C.; Zhang, X.; Zhang, Q. A Potential Target Associated with both Cancer and Cancer Stem Cells: A Combination Therapy for Eradication of Breast Cancer Using Vinorelbine Stealthy Liposomes Plus Parthenolide Stealthy Liposomes. *J. Controlled Release* **2008**, *129*, 18–25.

(17) Bartneck, M.; Scheyda, K. M.; Warzecha, K. T.; Rizzo, L. Y.; Hittatiya, K.; Luedde, T.; Storm, G.; Trautwein, C.; Lammers, T.; Tacke, F. Fluorescent Cell-Traceable Dexamethasone-Loaded Liposomes for the Treatment of Inflammatory Liver Diseases. *Biomaterials* **2015**, *37*, 367–382.

(18) Ozbakir, B.; Crielaard, B. J.; Metselaar, J. M.; Storm, G.; Lammers, T. Liposomal Corticosteroids for the Treatment of Inflammatory Disorders and Cancer. *J. Controlled Release* **2014**, *190*, 624–636.

(19) Monteiro, N.; Martins, M.; Martins, A.; Fonseca, N. A.; Moreira, J. N.; Reis, R. L.; Neves, N. M. Antibacterial Activity of Chitosan Nanofiber Meshes with Liposomes Immobilized Releasing Gentamicin. *Acta Biomater.* **2015**, *18*, 196–205.

(20) Kojima, M.; Zhang, Z.; Nakajima, M.; Ooe, K.; Fukuda, T. Construction and Evaluation of Bacteria-Driven Liposome. *Sens. Actuators, B* **2013**, *183*, 395–400.

(21) Monteiro, N.; Martins, A.; Pires, R. A.; Faria, S.; Fonseca, N. A.; Moreira, J. N.; Reis, R. L.; Neves, N. M. Dual Release of a Hydrophilic and a Hydrophobic Osteogenic Factor from a Single Liposome. *RSC Adv.* **2016**, *6*, 114599–114612.

(22) Li, X.-Y.; Zhao, Y.; Sun, M.-G.; Shi, J.-F.; Ju, R.-J.; Zhang, C.-X.; Li, X.-T.; Zhao, W.-Y.; Mu, L.-M.; Zeng, F.; Lou, J.-N.; Lu, W.-L. Multifunctional Liposomes Loaded with Paclitaxel and Artemether for Treatment of Invasive Brain Glioma. *Biomaterials* **2014**, *35*, 5591–5604.

(23) De Leo, V.; Mattioli-Belmonte, M.; Cimmarusti, M. T.; Panniello, A.; Dicarolo, M.; Milano, F.; Agostiano, A.; De Giglio, E.; Catucci, L. Liposome-Modified Titanium Surface: A Strategy to Locally Deliver Bioactive Molecules. *Colloids Surf., B* **2017**, *158*, 387–396.

(24) Mourtas, S.; Diamanti, G.; Foka, A.; Dracopoulos, V.; Klepetsanis, P.; Stamouli, V.; Spiliopoulou, I.; Antimisariis, S. G. Inhibition of Bacterial Attachment on Surfaces by Immobilization of Tobramycin-Loaded Liposomes. *J. Biomed. Nanotechnol.* **2015**, *11*, 2186–2196.

(25) Kastellorizios, M.; Michanetzis, G. P. A. K.; Pistillo, B. R.; Mourtas, S.; Klepetsanis, P.; Favia, P.; Sardella, E.; d'Agostino, R.; Missirlis, Y. F.; Antimisariis, S. G. Haemocompatibility Improvement of Metallic Surfaces by Covalent Immobilization of Heparin-Liposomes. *Int. J. Pharm.* **2012**, *432*, 91–98.

(26) Mourtas, S.; Kastellorizios, M.; Klepetsanis, P.; Farsari, E.; Amanatides, E.; Mataras, D.; Pistillo, B. R.; Favia, P.; Sardella, E.; d'Agostino, R.; Antimisariis, S. G. Covalent Immobilization of

Liposomes on Plasma Functionalized Metallic Surfaces. *Colloids Surf, B* **2011**, *84*, 214–220.

(27) Pasquardini, L.; Lunelli, L.; Vanzetti, L.; Anderle, M.; Pederzoli, C. Immobilization of Cationic Rifampicin-Loaded Liposomes on Polystyrene for Drug-Delivery Applications. *Colloids Surf, B* **2008**, *62*, 265–272.

(28) Monteiro, N.; Ribeiro, D.; Martins, A.; Faria, S.; Fonseca, N. A.; Moreira, J. N.; Reis, R. L.; Neves, N. M. Instructive Nanofibrous Scaffold Comprising Runt-Related Transcription Factor 2 Gene Delivery for Bone Tissue Engineering. *ACS Nano* **2014**, *8*, 8082–8094.

(29) Jensen, B. E. B.; Hosta-Rigau, L.; Spycher, P. R.; Reimhult, E.; Städler, B.; Zelikin, A. N. Lipogels: Surface-Adherent Composite Hydrogels Assembled from Poly(vinyl alcohol) and Liposomes. *Nanoscale* **2013**, *5*, 6758–6766.

(30) Lynge, M. E.; Laursen, M. B.; Hosta-Rigau, L.; Jensen, B. E. B.; Ogaki, R.; Smith, A. A. A.; Zelikin, A. N.; Städler, B. Liposomes as Drug Deposits in Multilayered Polymer Films. *ACS Appl. Mater. Interfaces* **2013**, *5*, 2967–2975.

(31) Cho, H.-j.; Perikamana, S. K. M.; Lee, J.-h.; Lee, J.; Lee, K.-M.; Shin, C. S.; Shin, H. Effective Immobilization of BMP-2 Mediated by Polydopamine Coating on Biodegradable Nanofibers for Enhanced *in Vivo* Bone Formation. *ACS Appl. Mater. Interfaces* **2014**, *6*, 11225–11235.

(32) Lee, H.; Dellatore, S. M.; Miller, W. M.; Messersmith, P. B. Mussel-Inspired Surface Chemistry for Multifunctional Coatings. *Science* **2007**, *318*, 426–430.

(33) Wen, X.; Wang, K.; Zhao, Z.; Zhang, Y.; Sun, T.; Zhang, F.; Wu, J.; Fu, Y.; Du, Y.; Zhang, L.; Sun, Y.; Liu, Y.; Ma, K.; Liu, H.; Song, Y. Brain-Targeted Delivery of Trans-Activating Transcriptor-Conjugated Magnetic PLGA/Lipid Nanoparticles. *PLoS One* **2014**, *9*, No. e106652.

(34) He, S.; Zhou, P.; Wang, L.; Xiong, X.; Zhang, Y.; Deng, Y.; Wei, S. Antibiotic-Decorated Titanium with Enhanced Antibacterial Activity through Adhesive Polydopamine for Dental/Bone Implant. *J. R. Soc., Interface* **2014**, *11*, No. 20140169.

(35) Garrido-Mesa, N.; Zarzuelo, A.; Gálvez, J. Minocycline: Far Beyond an Antibiotic. *Br. J. Pharmacol.* **2013**, *169*, 337–352.

(36) Norowski, P. A.; Babu, J.; Adatrow, P. C.; Garcia-Godoy, F.; Haggard, W. O.; Bumgardner, J. D. Antimicrobial Activity of Minocycline-Loaded Genipin-Crosslinked Nano-Fibrous Chitosan Mats for Guided Tissue Regeneration. *J. Biomater. Nanobiotechnol.* **2012**, *3*, 528–532.

(37) Li, Y.-F.; Rubert, M.; Yu, Y.; Besenbacher, F.; Chen, M. Delivery of Dexamethasone from Electrospun PCL–PEO Binary Fibers and Their Effects on Inflammation Regulation. *RSC Adv.* **2015**, *5*, 34166–34172.

(38) Kim, D.-H.; Martin, D. C. Sustained Release of Dexamethasone from Hydrophilic Matrices Using PLGA Nanoparticles for Neural Drug Delivery. *Biomaterials* **2006**, *27*, 3031–3037.

(39) Webber, M. J.; Matson, J. B.; Tamboli, V. K.; Stupp, S. I. Controlled Release of Dexamethasone from Peptide Nanofiber Gels to Modulate Inflammatory Response. *Biomaterials* **2012**, *33*, 6823–6832.

(40) Xing, C.; Levchenko, T.; Guo, S.; Stins, M.; Torchilin, V. P.; Lo, E. H. Delivering Minocycline into Brain Endothelial Cells with Liposome-Based Technology. *J. Cereb. Blood Flow Metab.* **2012**, *32*, 983–988.

(41) Wang, X.-X.; Li, Y.-B.; Yao, H.-J.; Ju, R.-J.; Zhang, Y.; Li, R.-J.; Yu, Y.; Zhang, L.; Lu, W.-L. The Use of Mitochondrial Targeting Resveratrol Liposomes Modified with a Dequalinium Polyethylene Glycol-Distearoylphosphatidyl Ethanolamine Conjugate to Induce Apoptosis in Resistant Lung Cancer Cells. *Biomaterials* **2011**, *32*, 5673–5687.

(42) Torchilin, V. P. Recent Advances with Liposomes as Pharmaceutical Carriers. *Nat. Rev. Drug Discovery* **2005**, *4*, 145–160.

(43) Dzieciuch, M.; Rissanen, S.; Szydłowska, N.; Bunker, A.; Kumorek, M.; Jamróz, D.; Vattulainen, I.; Nowakowska, M.; Róg, T.; Kepczynski, M. PEGylated Liposomes as Carriers of Hydrophobic Porphyrins. *J. Phys. Chem. B* **2015**, *119*, 6646–6657.

(44) Monteiro, N.; Martins, A.; Reis, R. L.; Neves, N. M. Liposomes in Tissue Engineering and Regenerative Medicine. *J. R. Soc., Interface* **2014**, *11*, No. 20140459.

(45) Eloy, J. O.; de Souza, M. C.; Petrilli, R.; Barcellos, J. P. A.; Lee, R. J.; Marchetti, J. M. Liposomes as Carriers of Hydrophilic Small Molecule Drugs: Strategies to Enhance Encapsulation and Delivery. *Colloids Surf, B* **2014**, *123*, 345–363.

(46) Akbarzadeh, A.; Rezaei-Sadabady, R.; Davaran, S.; Joo, S. W.; Zarghami, N.; Hanifehpour, Y.; Samiei, M.; Kouhi, M.; Nejati-Koshki, K. Liposome: Classification, Preparation, and Applications. *Nanoscale Res. Lett.* **2013**, *8*, 102.

(47) Song, Y.; Ye, G.; Wu, F. C.; Wang, Z.; Liu, S. Y.; Kopeć, M.; Wang, Z.; Chen, J.; Wang, J.; Matyjaszewski, K. Bioinspired Polydopamine (PDA) Chemistry Meets Ordered Mesoporous Carbons (OMCs): A Benign Surface Modification Strategy for Versatile Functionalization. *Chem. Mater.* **2016**, *28*, 5013–5021.

(48) Zhou, P.; Deng, Y.; Lyu, B.; Zhang, R.; Zhang, H.; Ma, H.; Lyu, Y.; Wei, S. Rapidly-Deposited Polydopamine Coating via High Temperature and Vigorous Stirring: Formation, Characterization and Biofunctional Evaluation. *PLoS One* **2014**, *9*, No. e113087.

(49) Shimomura, K.; Kanamoto, T.; Kita, K.; Akamine, Y.; Nakamura, N.; Mae, T.; Yoshikawa, H.; Nakata, K. Cyclic Compressive Loading on 3D Tissue of Human Synovial Fibroblasts Upregulates Prostaglandin E2 Via COX-2 Production without IL-1 β and TNF- α . *Bone Joint Res.* **2014**, *3*, 280–288.

(50) Vacanti, N. M.; Cheng, H.; Hill, P. S.; Guerreiro, J. D. T.; Dang, T. T.; Ma, M.; Watson, S.; Hwang, N. S.; Langer, R.; Anderson, D. G. Localized Delivery of Dexamethasone from Electrospun Fibers Reduces the Foreign Body Response. *Biomacromolecules* **2012**, *13*, 3031–3038.

(51) Alibetti, W.; Giarratana, L. S.; Viganò, C.; Castiglioni, S.; Maier, J. A. Sclerostin: A Novel Player Regulating Bone Mass in Inflammation? *Eur. J. Inflammation* **2013**, *11*, 345–352.

(52) Wang, Q.; Zhang, B.; Yu, J.-L. Farrerol Inhibits IL-6 and IL-8 Production in LPS-Stimulated Human Gingival Fibroblasts by Suppressing PI3K/AKT/NF-kB Signaling Pathway. *Arch. Oral Biol.* **2016**, *62*, 28–32.

(53) Doyle, C. J.; Fitzsimmons, T. R.; Marchant, C.; Dharmapatri, A. A. S. S. K.; Hirsch, R.; Bartold, P. M. Azithromycin Suppresses *P. gingivalis* LPS-Induced Pro-Inflammatory Cytokine and Chemokine Production by Human Gingival Fibroblasts *in Vitro*. *Clin. Oral Invest.* **2015**, *19*, 221–227.

(54) Agrawal, S.; Guess, A. J.; Chanley, M. A.; Smoyer, W. E. Albumin-Induced Podocyte Injury and Protection are Associated with Regulation of COX-2. *Kidney Int.* **2014**, *86*, 1150–1160.

(55) Morais, J. M.; Papadimitrakopoulos, F.; Burgess, D. J. Biomaterials/Tissue Interactions: Possible Solutions to Overcome Foreign Body Response. *AAPS J.* **2010**, *12*, 188–196.

(56) Zolnik, B. S.; Burgess, D. J. Evaluation of *in Vivo*–*in Vitro* Release of Dexamethasone from PLGA Microspheres. *J. Controlled Release* **2008**, *127*, 137–145.

(57) Smoak, K. A.; Cidłowski, J. A. Mechanisms of Glucocorticoid Receptor Signaling During Inflammation. *Mech. Ageing Dev.* **2004**, *125*, 697–706.

(58) Kaplan, J. B. Biofilm Dispersal: Mechanisms, Clinical Implications, and Potential Therapeutic Uses. *J. Dent. Res.* **2010**, *89*, 205–218.

(59) Maruyama, N.; Maruyama, F.; Takeuchi, Y.; Aikawa, C.; Izumi, Y.; Nakagawa, I. Intraindividual Variation in Core Microbiota in Peri-Implantitis and Periodontitis. *Sci. Rep.* **2014**, *4*, No. 6602.

(60) Hojo, K.; Nagaoka, S.; Ohshima, T.; Maeda, N. Bacterial Interactions in Dental Biofilm Development. *J. Dent. Res.* **2009**, *88*, 982–990.

(61) Yuan, S. J.; Pehkonen, S. O.; Ting, Y. P.; Neoh, K. G.; Kang, E. T. Inorganic–Organic Hybrid Coatings on Stainless Steel by Layer-by-Layer Deposition and Surface-Initiated Atom-Transfer-Radical Polymerization for Combating Biocorrosion. *ACS Appl. Mater. Interfaces* **2009**, *1*, 640–652.

(62) Costerton, J. W.; Stewart, P. S.; Greenberg, E. P. Bacterial Biofilms: A Common Cause of Persistent Infections. *Science* **1999**, *284*, 1318–1322.

(63) Lv, H.; Chen, Z.; Yang, X.; Cen, L.; Zhang, X.; Gao, P. Layer-by-Layer Self-Assembly of Minocycline-Loaded Chitosan/Alginate Multilayer on Titanium Substrates to Inhibit Biofilm Formation. *J. Dent.* **2014**, *42*, 1464–1472.

(64) Lu, H.; Liu, Y.; Guo, J.; Wu, H.; Wang, J.; Wu, G. Biomaterials with Antibacterial and Osteoinductive Properties to Repair Infected Bone Defects. *Int. J. Mol. Sci.* **2016**, *17*, 334.

(65) Connell, S. R.; Tracz, D. M.; Nierhaus, K. H.; Taylor, D. E. Ribosomal Protection Proteins and Their Mechanism of Tetracycline Resistance. *Antimicrob. Agents Chemother.* **2003**, *47*, 3675–3681.

(66) Chopra, I.; Roberts, M. Tetracycline Antibiotics: Mode of Action, Applications, Molecular Biology, and Epidemiology of Bacterial Resistance. *Microbiol. Mol. Biol. Rev.* **2001**, *65*, 232–260.